

DDPG car-following model with real-world human driving experience in CARLA

Dianzhao Li^a, Ostap Okhrin^a

^a*The Institute of Transport and Economics, Dresden University of Technology, 01062, Dresden, Germany*

Abstract

In the autonomous driving field, the fusion of human knowledge into Deep Reinforcement Learning (DRL) is often based on the human demonstration recorded in the simulated environment. This limits the generalization and the feasibility of application in real-world traffic. We proposed a two-stage DRL method, that learns from real-world human driving to achieve performance that is superior to the pure DRL agent. Training a DRL agent is done within a framework for CARLA with Robot Operating System (ROS). For evaluation, we designed different real-world driving scenarios to compare the proposed two-stage DRL agent with the pure DRL agent. After extracting the 'good' behavior from the human driver, such as anticipation in a signalized intersection, the agent becomes more efficient and drives safer, which makes this autonomous agent more adapt to Human-Robot Interaction (HRI) traffic.

Keywords: Deep reinforcement learning, Car-following model, Real driving dataset, CARLA, ROS

1. Introduction

With the vigorous development of new energy vehicles, autonomous driving has become more and more attractive to academia. Due to the complex real-world traffic environment, vehicles are making continuous decisions that are building cornerstones in achieving fully autonomous driving. A list of solutions for complex decision-making problems has been proposed in the literature over the last decades.

The first family of autonomous techniques is the so-called *rule-based* control strategies, which use lists of complex control rules to define the behavior of vehicles in the traffic flow. As an example, for the car-following task in autonomous

driving, models worth mentioning are the Gaxis-Herman-Rothery (GHR) model by Gazis et al. (1961), the Wiedemann (1974) car-following model, Intelligent Driver Model (IDM) by Treiber et al. (2000) or stochastic car-following models by Treiber and Kesting (2017). Kikuchi and Chakroborty (1992) proposed a fuzzy inference system-based car-following model, which consists of many straightforward natural language-based driving rules. Obviously, it is impossible to consider all the conditions that may occur and formulate corresponding control strategies accordingly. Namely, rule-based control strategies are unfit for the time-varying and non-stationary traffic conditions. Furthermore, most of the current autonomous driving control policies are based on the sensor facilities placed on the car, such as Global Navigation Satellite System (GNSS), Light Detection and Ranging (LiDAR), Camera, etc. This means that car behavior heavily depends on the quality of the information obtained from receivers and needs to make a correct decision even under sensor failure and unavailability for some scenarios. For instance, GNSS may not always be available because of the effects of signal attenuation and signal occlusion problems. One of the traditional solutions is to install multiple different sensors on the car to form redundancy. This is valuable in the situation when a single sensor may not be available but imply an increase in cost.

Due to the rapid development of deep learning in recent years, another approach to solve control problems involves the use of *imitation learning* or *behavior cloning*. With the behavior cloning method, the perception and control parts in autonomous driving are learned from human demonstrations using deep neural networks (DNN). The DNN learn, with an RGB image from the camera as input, outputs the desired reaction to the vehicle control in certain circumstances. Moreover, end-to-end imitation systems can be learned offline in a safe way. Bojarski et al. (2016) trained a convolutional neural network (CNN) to map raw images from a single camera directly to steering commands. Codevilla et al. (2018) proposed command-conditional imitation learning, in which low-level controls, as well as high-level commands, learned from expert demonstrations with vision-based inputs.

Although behavioral cloning is widely used, even in real cars, that are allowed for driving on the streets, it still has many shortcomings. Codevilla et al. (2019) pointed out that four main limitations to be considered:

Generalization: As a type of supervised learning, behavior cloning is also limited by the size of the dataset and scenarios that are not covered by the dataset. This means in scenarios that do not appear in the dataset, the performance will be unsatisfactory.

Driving dataset biases: Supervised learning is limited by the type or the source of the dataset, and the trained control strategy will be biased. Diversity is an important criterion for a dataset, as every driver has his own driving style, and even different vehicles have different driving performances, which are reflected in the datasets (Codevilla et al., 2019). The fairness in machine learning (Barocas et al., 2017) is still an unsettled problem.

Causal confusion: It is shown that some spurious correlations cannot be distinguished from true causes in human demonstration patterns if we do not use an explicit causal model or on-policy demonstrations, see de Haan et al. (2019).

High variance: Since off-policy imitation learning uses a static dataset, initialization and data sampling will induce high variance. As the cost function in behavior cloning is optimized via Stochastic Gradient Descent (SGD), which assumes the data is independent and identically distributed. However, the human demonstration dataset is usually interrelated over a long period of time. Therefore the model can be very sensitive to the initialization (Hanin and Rolnick, 2018).

Another feasible solution that has attracted widespread attention in the academic community over the last decades is *Deep Reinforcement Learning* (DRL). DRL that combines reinforcement learning and deep learning, has provided solutions for many complex decision-making tasks on playing chess, Go, Atari games, uses in robotics, drones, and vehicle behavior (Mnih et al., 2013; Silver et al., 2016; Silver et al., 2017; Gu et al., 2017; Akhloufi et al., 2019; He et al., 2017; Isele et al., 2018). Within this field, agents interact with the environments to learn the optimal behaviors, improving over time through reward and error.

As for the applications of DRL in traffic, Sallab et al. (2016) used Deep Q learning (DQN) and Deep Deterministic Actor Critic Algorithm (DDAC) as control algorithms for lane keeping tasks in TORCS simulator. Later, Wang et al. (2018) proposed Q-learning based training process to train a control policy for lane changing tasks with a smooth and efficient behavior. The study by Ngai and Yung (2011) offered a multiple-goal reinforcement learning framework, which is used to solve the overtaking problem in traffic flow with correct action as well as collision avoidance. Recently, Nosrati et al. (2018) proposed an RL-based hierarchical framework with DQN and Proximal Policy Optimization (PPO) to solve the multi-lane cruising problem, it shows that this design enables better learning performance.

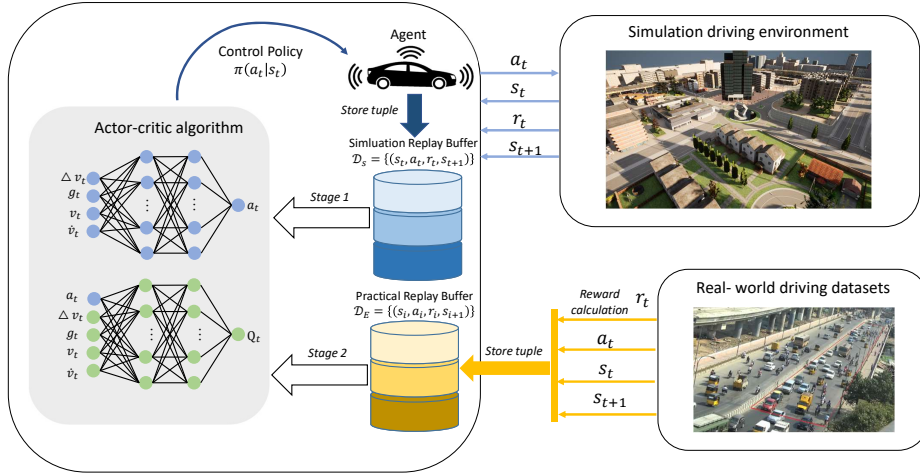


Figure 1: The conceptual framework of the two-stage DDPG agent. Stage 1: the agent updates networks with the simulation replay buffer. Stage 2: the agent learns from the modified practical replay buffer based on real driving datasets.

In addition to pure DRL, researchers are combining DRL with human prior knowledge to improve training efficiency. Vecerik et al. (2017) proposed a method to use human demonstrations with Deep Deterministic Policy Gradient (DDPG) algorithm. The human demonstrations and actual interactions are filled into the replay buffer and sampled with prioritized replay mechanism. The results on simulated tasks show that DDPG with demonstrations outperforms pure DDPG. Huang et al. (2021) proposed a framework that first uses behavioral cloning with the expert demonstration to derive an imitative expert policy and then further improve it with DRL. A different approach has been done by Liu et al. (2021) who modified the update of the policy network in RL to leverage human prior knowledge, which can adaptively sample experience from the agent’s self-exploration and expert demonstration for the policy update. In the next, we briefly outline our contribution.

1.1. Contribution

Even possessing methods combining human demonstrations with DRL, the following limitations need to be treated with care:

1. As stated in the introduction, most of the papers combining the human demonstrations with DRL, the human demonstrations are generated and

recorded in a simulated or a limited real environment. This leads to restrictions on generalization and dataset biases issues when using the data.

2. While training a DRL agent, the behaviors of the agent depend heavily on the reward function, which is generally defined by researchers based on experience. This type of definition does not guarantee that the actions of the trained agent are completely safe or comfortable, what implies that the agent trained solely on the reward function is not perfect.
3. While using human demonstrations, there is no guarantee that every action of the human expert is perfect and that there is no other better action. Therefore, the choice of expert data is another issue that needs attention.
4. Recording data usually requires tens of hours of operations by human experts, which is very resource-intensive. Even collected with the best patience, data is always contaminated with errors.

One of the biggest challenges we faced in this project is the problem of balancing the policies learned by the agent itself through DRL and the policies in the human demonstration for better control policies. Moreover, we consider an important challenge for developing autonomous car-following DRL agents with real-world datasets instead of human demonstrations in simulated environments.

The overall system architecture is depicted in Figure 1. First, we use DRL to train an agent that can follow the leading vehicle and maintain the desired distance and speed as well to ensure comfort. Second, we add real driving datasets into the experience replay buffer and resume training the agent. The reason for this order lies in the hope that the agent can extract some good human driving policies from the dataset, and further improve its driving behavior which is better adapted to the real driving environment. As an example consider anticipation in traffic: in many cases, the driver notices what is happening in front of the leader vehicle, this allows the driver to adjust his driving behavior. For example, do not brake completely seeing for a long time red traffic light, anticipating change to the green. Furthermore, we propose a novel framework that uses CARLA and Robot operating system (ROS) for co-simulation to deal with the communication problem among multiple vehicles.

The remainder of this paper is organized as follows. In Section 2, the preliminary knowledge related to this work is reviewed. Then, we introduce our approach in detail in Section 3 and the experimental setups for training and evaluation process are discussed in Section 4. Afterwards, we evaluate the trained agents with

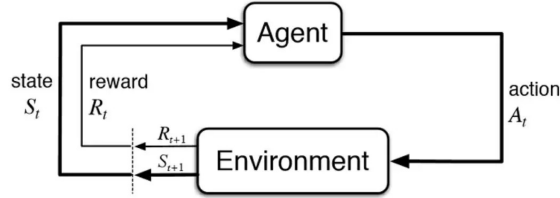


Figure 2: A reinforcement learning agent learns its action policy by interacting with the environment.

different driving scenarios and discuss the results in Section 5. Section 6 summarizes this paper.

2. Related works

2.1. Reinforcement Learning

The Reinforcement Learning (RL) process is considered as a Markov Decision Process (MDP), an autonomous agent at time step t observes a state s_t of the environment. It interacts with the environment by taking an action a_t according to the policy $\pi(a_t|s_t)$. After the action is executed by the agent, the environment and the agent transition to a new state s_{t+1} and a reward r_{t+1} is provided to the agent as the feedback. New state s_{t+1} depends on the current state s_t and the chosen action a_t with transition probability $P(s_{t+1}|s_t, a_t)$. The RL process is shown simplistically in Figure 2.

The objective is to find the optimal policy π^* that maximizes the expected discounted cumulative rewards

$$R_t = r_{t+1} + \gamma r_{t+2} + \gamma^2 r_{t+3} + \dots = \sum_{k=0}^{\infty} \gamma^k r_{t+k+1}, \quad (1)$$

where $\gamma \in [0, 1]$ is the discount factor and lower values mean the agent prefers immediate to distant rewards. Furthermore, in RL we use a state-value function $V^\pi(s_t)$ to measure how good a certain state s_t is, in terms of expected cumulative reward by following a certain policy π :

$$V^\pi(s_t) = \mathbb{E}_\pi \{R_t | s_t\}. \quad (2)$$

Similarly, the action-value function $Q^\pi(s_t, a_t)$ is defined as the expected return starting from s_t , taking the action a_t , and thereafter following policy π :

$$Q^\pi(s_t, a_t) = \mathbb{E}_\pi \{R_t | s_t, a_t\}. \quad (3)$$

Although RL can come up with some optimal policy after training, for the large state and action space in high dimensions, such a tabular format becomes computationally infeasible. Especially the real-world problems usually have uncountable state space in high dimensions. This challenge has plagued researchers for a long time, which has led to the stagnation of the development of RL. With the development of deep learning, DRL regained the interest of academia with DNN being used to approximate the optimal Q values. The classical success story is Mnih et al. (2015) who first proposed a deep Q-network (DQN) method. With this method, the agent performs at a level comparable and often superior to a professional human player in Atari video games. Later Silver et al. (2016) proposed a new approach for the Go game. Two deep neural networks were used: one value network to evaluate board positions and another is policy network to select moves. These two networks are first trained by supervised learning with human expert knowledge, and then use RL for further training. This was the first time computer defeated a human professional player in Go.

Although DQN solves problems with high-dimensional observation spaces, it can only handle discrete and low-dimensional action spaces. Lillicrap et al. (2015) developed a Deep deterministic policy gradient (DDPG) method that can learn policies in high-dimensional, continuous action spaces. DDPG is an actor-critic algorithm with two networks: actor network $\mu(s|\theta^\mu)$ with network parameter θ^μ and critic network $Q(s, a|\theta^Q)$ with network parameter θ^Q . The actor network will output an action a_t based on the given states s_t , the critic network gets the action a_t from the actor network, and the given states s_t , predict the goodness of the action a_t . Similar to DQN, DDPG also uses the target networks method with the target actor network μ' and target critic network Q' . Lillicrap et al. (2015) found that for more stable learning, it is better to make the target networks slowly track the trained networks. The parameters of the target networks after each update of the trained network are updated using a sliding average for both the actor and the critic:

$$\theta^{\mu'} = \tau\theta^\mu + (1 - \tau)\theta^{\mu'}, \quad (4)$$

$$\theta^{Q'} = \tau\theta^Q + (1 - \tau)\theta^{Q'}, \quad (5)$$

where $\tau \ll 1$ is the soft target update rate.

As the policy in DDPG is deterministic, it can very quickly produce the same

actions, which may lead to missing some rewarding options, therefore, the balance between exploration and exploitation becomes an issue. The solution retained in DDPG is an additive noise added to the deterministic action to explore the action space:

$$a_t = \mu(s_t | \theta^\mu) + \xi_t. \quad (6)$$

This additive noise ξ could be the realization of the Gaussian distribution or the zero-reverting Uhlenbeck and Ornstein (1930) process suggested by Lillicrap et al. (2015). Ornstein-Uhlenbeck processes are used in physics or finance to model the velocity of Brownian particles with frictions or evolution of prices. It updates a variable z_t using a stochastic differential equation (SDE):

$$dz_t = -\theta_n z_t dt + \sigma_n dW_t, \quad (7)$$

where $\theta_n > 0$, $\sigma_n > 0$ are parameters, W_t denotes the Wiener process.

The pseudo-algorithm of DDPG is shown in Algorithm 1.

2.2. Experience replay

If the networks only learned the highly correlated consecutive samples from the experience as they occurred sequentially in the environment, this would therefore lead to inefficient learning. One possible approach to solve this problem involves the use of *experience replay* proposed by Lin (1992). Following it we store the experiences of an agent at each time step in a dataset called the *replay memory*. Let us represent the experience of an agent at time t as d_t . At time step t , the experience is defined as a tuple:

$$d_t = (s_t, a_t, r_t, s_{t+1}), \quad (8)$$

containing the state of the environment s_t , the action a_t from agent at given state, the reward r_t the agent received as a result of the previous state-action pair (s_t, a_t) , and the next state of the environment s_{t+1} . A list of N tuples d_t will be saved in the *replay memory* D_t . With this replay buffer, we randomly sample some tuples that break the temporal correlations by mixing less recent experience for the updates, and rare experiences will be used for more than just a single update.

2.3. CARLA

CARLA is an open-source simulator grounded on Unreal Engine with hyper-realistic physics and uses the OpenDRIVE standard to define roads and urban settings (Dosovitskiy et al., 2017; Dupuis et al., 2010). It is based on a scalable

Algorithm 1: DDPG algorithm

Initialize actor network μ and critic network Q with random weights θ^μ and θ^Q

Initialize the target networks μ' and Q' with weights $\theta^{\mu'} \leftarrow \theta^\mu$, $\theta^{Q'} \leftarrow \theta^Q$

Initialize replay buffer D

for $episode \in [1, M]$ **do**

- Initialize a random process noise ξ for action exploration
- Receive initial observation state s_1
- for** $t \in [1, T]$ **do**
 - Select action $a_t = \mu(s_t | \theta^\mu) + \xi_t$ according to the current policy and exploration noise
 - Execute action a_t and observe reward r_t and observe new state s_{t+1}
 - Store transition (s_t, a_t, r_t, s_{t+1}) in D
 - Sample a random minibatch of N transitions (s_i, a_i, r_i, s_{i+1}) from D
 - Set $y_i = r_i + \gamma Q' \left\{ s_{i+1}, \mu'(s_{i+1} | \theta^{\mu'}) | \theta^{Q'} \right\}$
 - Update critic by minimizing the loss:
$$L = \frac{1}{N} \sum_i \{y_i - Q(s_i, a_i | \theta^Q)\}^2$$
 - Update the actor policy using the sampled policy gradient:
$$\nabla_{\theta^\mu} J \approx \frac{1}{N} \sum_i \nabla_a Q(s, a | \theta^Q) \Big|_{s=s_i, a=\mu(s_i)} \nabla_{\theta^\mu} \mu(s | \theta^\mu) \Big|_{s_i}$$
 - Update the target networks:
$$\theta^{\mu'} = \tau \theta^\mu + (1 - \tau) \theta^{\mu'}$$
$$\theta^{Q'} = \tau \theta^Q + (1 - \tau) \theta^{Q'}$$

end

end

client-server architecture, with the server being responsible for simulation tasks, e.g. sensor rendering, computation of physics, etc. The client is usually defined by the user, which can easily specify via API the sensor setup of the vehicle. Afterwards, a controlled amount of camera images and vehicle-related information will be provided for further usage. Because of the high-fidelity of CARLA, it is often used in the field of autonomous driving (Ravi Kiran et al., 2018; Dworak et al., 2019; Gómez-Huélamo et al., 2020; Tran and Le, 2019; Niranjana et al., 2021). Furthermore, CARLA also provides the CARLA-ROS bridge that enables two-way communication between Robot Operating System (ROS) (Quigley et al., 2009) and CARLA.

ROS is an open-source robotics middleware suite, which enables the communication between various sensors on a single robot and multiple robots without affecting the independence of each part. Since automated vehicles are complex systems with a high degree of interdependencies between their components, ROS is suitable for us to carry autonomous driving tasks such as car-following, to realize the communication between leader and follower, and it does not affect the individual control strategy of each vehicle (Hellmund et al., 2016).

3. Our approaches

3.1. System overview

As shown in Figure 1, we train and evaluate our control policies directly using the CARLA simulator. Agent interacts with the simulation environment to obtain rewards, observe the states, and store them in the replay buffer. Therefore we update the DNN with the small batches sampled from the replay buffer. Here, we assume that the states observed by the agent are already known, including the position of the leader and follower, velocity, acceleration, and other information, since this only involves simple sensor information processing issues which is out of the scope of the current research. After training the DRL agent, we store the processed real driving data set into another replay buffer called the practical replay buffer and continue training the agent. The system control policy is composed of two parts, which are longitudinal (acceleration) control policy with DRL agent and lateral (steering) control policy with Stanley controller.

3.2. DDPG agent for longitudinal control

In this paper, we use DDPG discussed in Section 2.1 as our working DRL algorithm to obtain the longitudinal control policy. The setup of the DDPG algorithm will be introduced in this section. Since the main intention of this paper is

to improve the existing RL agent with human experience data, we do not consider other algorithms.

3.2.1. Action and state space

For the action space A of DDPG, we choose continuous variable acceleration. The reasons for choosing acceleration are as follows:

- In the case of the end-to-end DRL algorithm, the action space is the throttle and brake. Although this can potentially solve the internal control problem of the vehicle, it is accompanied with the decrease in generalization. Different vehicles have different dynamic characteristics, therefore this setting makes our algorithm useful for fixed vehicles and cannot be applied to other types.
- The real human driving data we use comes from the platoon driving experiments of Punzo et al. (2005). This driving data does not contain direct information about throttles and brakes, but the speed and acceleration. If we want to use real driving data, it is more conducive to using acceleration as action space.

To follow the leader, the agent needs to be able to communicate with it, so as the state space S , we use such features as the velocity of follower v_t , the acceleration of follower \dot{v}_t , the leader's velocity $v_{t,l}$, and the bumper-to-bumper gap g_t . Moreover, as suggested by Kim (1999), we normalize the data generally for speeding up the learning process and faster convergence. The state s_t at time step t is defined as

$$s_t = \begin{pmatrix} \frac{v_t}{v_{des}} \\ \frac{\dot{v}_t - \dot{v}_{min}}{\dot{v}_{max} - \dot{v}_{min}} \\ \frac{v_{t,l} - v_t}{v_{des}} \\ \frac{g_t}{g_{max}} \end{pmatrix}, \quad (9)$$

where v_{des} denotes the desired speed, \dot{v}_{max} and \dot{v}_{min} define the feasible range of accelerations, g_{max} indicates the maximum space gap.

3.2.2. Reward function

As the most critical part of the RL algorithm, the formulation of the reward function is highly related to the performance of the agent. We choose the reward

function proposed by Hart et al. (2021), with which, the trained agent performs greatly in the car-following task. The reward function focuses on safety factor and also make a balance between the comfort for the driver and the driving efficiency. It can be divided into three weighted sub-rewards:

$$r_t = w_{safe}r_{t, safe} + w_{gap}r_{t, gap} + w_{jerk}r_{t, jerk}. \quad (10)$$

The first term $r_{t, safe}$ compares the kinematically needed deceleration with the comfortable deceleration b_{comf} and focuses on the response of driver to safety-critical situations:

$$r_{t, safe} = \begin{cases} -\tanh\left(\frac{b_{kin}-b_{comf}}{-\dot{v}_{min}}\right), & \text{if } b_{kin} > b_{comf}, \\ 0, & \text{otherwise,} \end{cases}$$

where

$$b_{kin} = \begin{cases} \frac{v_t - v_{t,l}}{g_t}, & \text{if } v_t > v_{t,l}, \\ 0, & \text{otherwise.} \end{cases}$$

The second term $r_{t, gap}$ devises for driving efficiency, to prevent the follower agent from keeping a long distance with the leader to avoid the occurrence of dangerous situations:

$$r_{t, gap} = \begin{cases} \frac{\varphi\{(g_t - g_{opt})/g_{var}\}}{\varphi(0)}, & \text{if } g_t < g^*, \\ \frac{\varphi\{(g_t - g_{opt})/g_{var}\}}{\varphi(0)} \left(1 - \frac{g_t - g^*}{g_{lim} - g^*}\right), & \text{otherwise,} \end{cases}$$

where

$$\begin{aligned} g_{opt} &= v_t T + g_{min}, \\ g_{var} &= 0.5g_{opt}, \\ g_{lim} &= v_t T_{lim} + 2g_{min}. \end{aligned}$$

The third term $r_{t, jerk}$ addresses the control of jerk for a comfortable driving:

$$r_{t, jerk} = -\left(\frac{1}{j_{comf}} \frac{d\dot{v}_t}{dt}\right)^2.$$

We choose the weights for safety factor $w_{safe} = 1.0$, efficiency factor $w_{gap} =$

0.5 and the comfortable factor weights $w_{jerk} = 0.004$ and rest hyperparameters as suggested by Hart et al. (2021) which were shown in Table 1.

Symbol	Description	Value
\dot{v}_{min}	Minimum acceleration	-9 m/s^2
\dot{v}_{max}	Maximum acceleration	5 m/s^2
v_{des}	Desired velocity	20 m/s
g_{max}	Maximum distance between leader and follower	200 m
b_{comf}	Comfortable deceleration	2 m/s^2
T	Desired time gap to the leading vehicle	1.5 s
g_{min}	Desired minimum space gap	2 m
T_{lim}	Upper time gap limit for zero reward	15 s

Table 1: Hyperparameters used for the input states and reward function setup.

3.2.3. Neural network structure

The structure of DDPG neural networks used in this study is depicted graphically in Figure 3. Both actor and critic are using fully connected neural networks with two hidden layers, both hidden layers contain 32 neurons. In two hidden layers, we use ReLU activation function. For the output layer in critic network, we use linear activation function, and for the output layer in actor network, we use *Tanh* as activation function to scale the output to $[-1, 1]$ for better performance, afterwards, this bounded output will be mapped to the acceleration range.

3.3. Lateral control policy

In the car-following task, we use a DRL agent for longitudinal control, but because of the high fidelity of physic parameters in the CARLA simulator, during the training, there were frictions between the tires and the road, which may cause very small heading drift error. As the training went on, the drift grew with time, usually 0.5° for 1000 training steps. To correct this heading drift error, we apply a lateral control policy (steering angle) to keep the vehicle in the middle of the road. In this paper, we use the Stanley controller proposed by Thrun et al. (2006). The considered controller is one type of geometrical path-tracking controllers, which helped Stanford to win the DARPA challenge in 2006. Moreover, since it considers both the lateral and the heading error, it shows a very good performance. In a Stanley controller, the steering angle ϕ_t of the vehicle is given by:

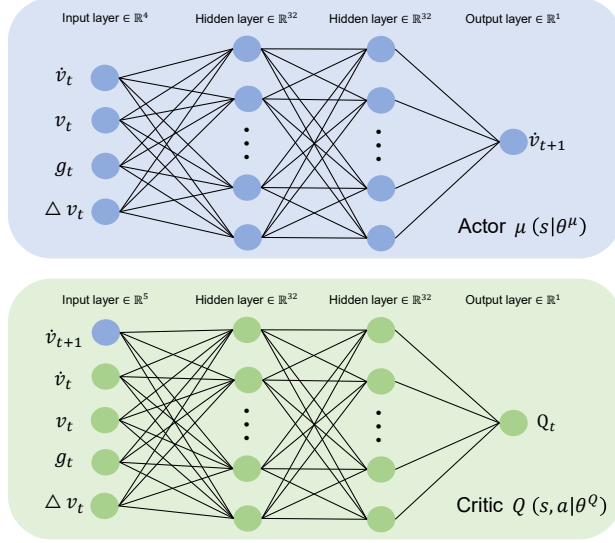


Figure 3: Neural network architecture of Actor and Critic in DDPG, each of them has two hidden layers with 32 neurons in each layer.

$$\phi_t = \theta_{p,t} + \tan^{-1} \left\{ \frac{d_{f,t}}{l_d} \right\},$$

where the first term compensates the angular error θ_{p_ϵ} and the second compensates the front lateral distance error d_{f_ϵ} measured from the center of the front axle to the nearest point on the path. Furthermore, l_d is a headway distance, which is usually chosen proportional to vehicle speed as $l_d = \frac{v}{k_v}$ and k_v is a normalizing constant.

Then the steering angle results in:

$$\phi_t = \theta_{p,t} + \tan^{-1} \left\{ \frac{k_v d_{f,t}}{v} \right\}.$$

3.4. Real-world human driving datasets

In this paper, we use the real-world car-following trajectory from Punzo et al. (2005), which we later on call "Napoli datasets". It is created and processed after a platoon driving experiment, in which several vehicles follow each other on urban roads and highways. The Napoli datasets were collected on two days along the same route on two urban roads and one rural road. It consists of five sub-dataset

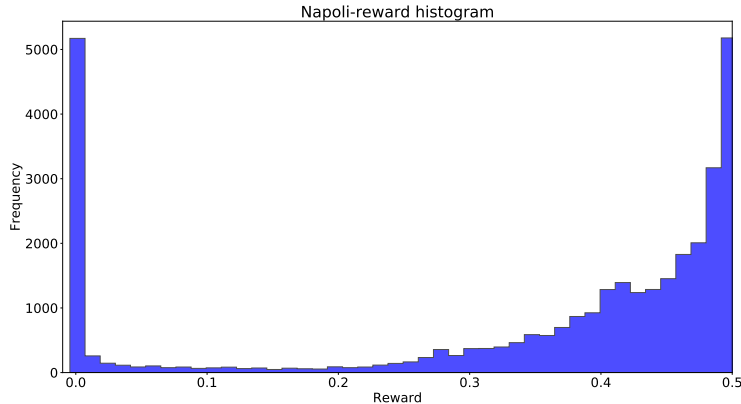


Figure 4: Reward distribution in Napoli datasets according to the reward function in Section 3.2.2.

with an overall amount of 24 min driving data. The first urban road is an 2 km long straight road with congested traffic (i.e., stop-and-go traffic conditions). It has four intersections and an estimated capacity of 900 vehicles per hour (veh/h). The second urban road is also approximately 2 km long but with an estimated capacity of 1200 veh/h. The rural road is a two-lane 3 km long highway with an estimated capacity of 1500 veh/h. The traffic flow during collecting datasets was approximately 400 veh/h. With a non-stationary Kalman filter (Kalman, 1960) applied to position data, high-quality car-following data was provided, including the velocity of each vehicle and bumper-to-bumper distance between leader-follower pair with the frequency of 10 Hz.

To store the driving datasets into replay buffer, we need to construct lists of tuples (s_i, a_i, r_i, s_{i+1}) . Since the states and action at each time step are already known from the datasets, only missing are the rewards. To compute the reward for each action the human driver made, we use the same reward function (10) as for the DDPG agent. The histogram of the resulted rewards for the human drivers is shown in Figure 4. As the maximum reward r_t agent can obtain is 0.5, we see that under this reward function setting, half of the actions performed by the human driver can be considered good and above ($r_i \geq 0.4$). This means that we can expect that the agent will learn some good behaviors from human drivers. Nevertheless, we still observe a large fraction of actions with zero reward.

4. Experimental setup

4.1. Simulation environment

As discussed in Section 2.3, we use CARLA being our simulation environment. Since CARLA is grounded on Unreal engine, the static objects like infrastructure, buildings, or vegetation, and dynamic objects such as vehicles, cyclists, or pedestrians are made by 3D models. All the 3D models are using low-weight geometric models and textures while maintaining visual realism due to a variable level of detail and carefully crafting the materials.

For the car-following task, we just need leading and following vehicles running on the road. To save computing resources and speed up the algorithms, we choose the OpenDRIVE standalone mode of CARLA for simulation. The standalone mode runs the full simulation by using only the OpenDRIVE file which describes every detail on the road. Other additional geometries or assets such as buildings or vegetation will not be created, as shown in Figure 5. The simulator will take the OpenDRIVE *.xodr* file and procedurally create temporal 3D meshes which describe the road definition in a minimalistic manner. Moreover, to prevent vehicles from falling off the road, visible walls are created at the boundaries of the road, to act as a safety measure.

4.2. CARLA-ROS co-simulation

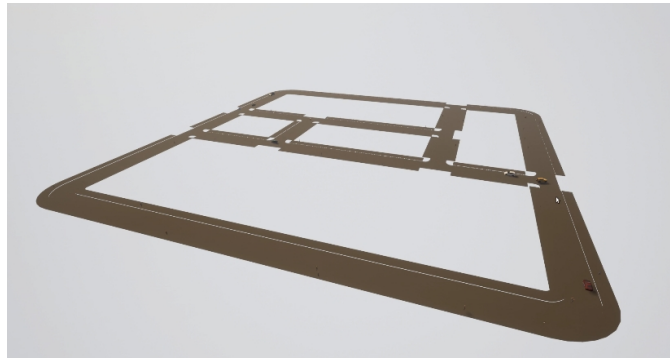
In this paper, we use CARLA-ROS co-simulation to implement and evaluate our approach. CARLA is a hyper-realistic simulated environment, which provides API to modify all aspects related to the simulation. However, to process the sensor information and enable interoperability with control and perception modules, we should rely on ROS. For the car-following task, we need to ensure the communication between leader and follower, which ROS has strength at (Hellmund et al., 2016). Furthermore, ROS provides GUI tools for diagnostics and monitoring during the development and run-time of the system. This allows us to have an immediate overview of the status of the system.

The transmission of information between two vehicles as well as the control node in ROS is realized via a transport system with *publish / subscribe* semantics. The control node can obtain required information from each vehicle, and publish control information to the agent, for instance, throttle and brake.

Here, *hero1* indicates the leader, and *hero2* means the follower in a leader-follower pair. Four different topics provide different information about the vehicles in CARLA:



(a) The common driving environment



(b) The OpenDRIVE standalone mode

Figure 5: Two different driving simulation modes of CARLA: (a) the standard driving mode in CARLA with full rendering; (b) the OpenDRIVE standalone mode with minimalistic rendering leads to better simulation efficiency.

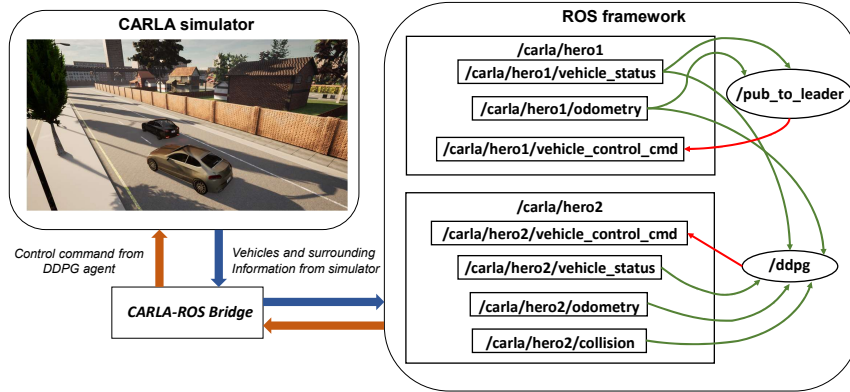


Figure 6: The structure of our proposed CARLA-ROS framework, the CARLA-ROS bridge transport the information of vehicles and surrounding from CARLA into ROS, afterward, transfer the control command from DDPG agent in ROS to the vehicle in CARLA.

1. */carla/hero/vehicle_status*: provides the current speed, acceleration, orientation of the vehicle, as well as the control values reported by CARLA.
2. */carla/hero/odometry*: provides the current position of the vehicle in the specified coordinate frame which usually is Cartesian coordinates (UTM).
3. */carla/hero/vehicle_control_cmd*: messages sent to CARLA apply a control signal to the vehicle, which includes throttle: [0.0, 1.0], brake: [0.0, 1.0], steering: [-1.0, 1.0].
4. */carla/hero/collision*: retrieves collision data detected by the collision sensor. It is used to reset the environment when a collision between two vehicles occurs.

As discussed in Section 3.2 and shown in Figure 6, neural networks that were updated and learned will output a control signal, such as acceleration of the agent, and will be transported back to CARLA to control the agent. However, in CARLA, there is no controller to directly use acceleration or speed to control vehicles. This can be performed indirectly via throttle and brake. For this reason, we use the reverse data method to obtain a controller that controls vehicles via acceleration and speed, as discussed in details in the next section.

4.3. Controller for CARLA

For CARLA simulation, */carla/hero/vehicle_control_cmd* topic is used to control the vehicle via throttle and brake. But as discussed in Section 4.2, we should

use acceleration as the output of our agent to ensure generalization. To overcome this problem, there are two feasible solutions: First, as vehicle models in CARLA are wrappers for the PhysX Vehicle by NVIDIA GameWorks, we can map the throttle and brake to velocity and acceleration with lists of equations according to the vehicle dynamic models. Nevertheless, in many cases, we can not use this method, when the dynamic models of the object are unknown. Second, we can use the reverse data method to train a simple neural network that links acceleration and velocity to throttle and brake. In this paper to allow for generally, we go for the second approach.

At first, we run four hours of driving test with automatic control mode in CARLA. In this case, the vehicle is controlled automatically by CARLA with throttle and brake. During the driving, we collect datasets that include the velocity and acceleration of the vehicle at each time step, as well as the throttle and brake at the same time step that result in the corresponding acceleration and velocity. At second, we reorganized the collected dataset with the input states:

$$x_t = \begin{pmatrix} v_{t+1} \\ v_t \\ a_t \end{pmatrix},$$

where v_{t+1} is the target velocity of next time step, v_t is the current velocity, a_t is the current acceleration. The output states of the neural network are:

$$y_t = \begin{pmatrix} g_t \\ b_t \end{pmatrix},$$

where g_t and b_t are throttle and brake at time step t respectively. This procedure can be performed with any other simulation environment.

We use a simple fully connected neural network as shown in Figure 7, and train it with the new reorganized dataset. Afterwards, if we want to apply the DDPG algorithm to different models of vehicles, only this control neural network should be retrained. As an example, if we have a robot car in the real world, but the actual physic models are unknown. We can first collect the controlling data similarly as in CARLA, and then train the control network with the input of acceleration. Afterwards, this extra control network can be connected to our pretrained DRL policy network and resume training for some small episodes to achieve sufficient performance. Compared with the end-to-end DRL, this method greatly improves generalization.

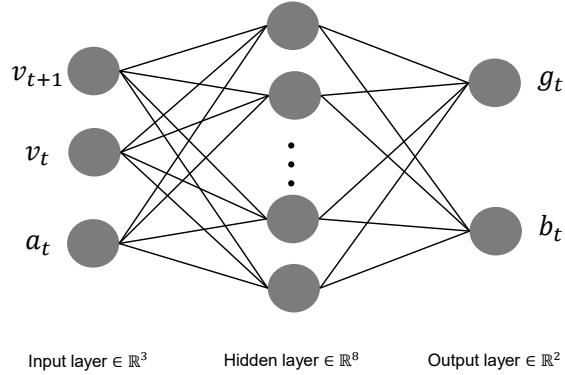


Figure 7: Control neural network with inputs of v_{t+1} , v_t , a_t , and output g_t and b_t .

Moreover, DRL needs to continuously interact with the environment to obtain rewards and optimize its policy, which means that in the autonomous driving area, it is impossible to train DRL agents in the real environment. CARLA provides the possibility to modify the physical parameters of the vehicle, thus, we can easily train the agent using the real vehicle parameters in CARLA and apply it seamlessly to the real world with greatly improved efficiency.

4.4. Training process

To train a car-following agent, we need a leader-follower pair. We use another Ornstein-Uhlenbeck process to generate a completely random leader trajectory according to the suggestion by Hart et al. (2021). As shown in Figure 6, the ROS node *pub_to_leader* receives the information from the leading vehicle and generates the next time step velocity v_{t+1} to control the leading vehicle.

To balance exploration and exploitation, we add exploration noise to the output of the DDPG policy network, and we will use clipping to ensure that the processed output does not exceed the boundary. In this paper, we use the zero-reverting Ornstein-Uhlenbeck process in (7) as exploration noise. The structure of actor and critic neural networks is discussed in Section 3.2.3. Before training our DDPG agent, we carefully choose a list of hyperparameters for the learning as shown in Table 2.

The training process runs on an NVIDIA GeForce RTX 3080 GPU and takes roughly two hours to finish 10000 steps of interaction with the simulated environment. The simulation interval is 0.1 seconds, which means the RL agent makes decisions every 0.1 seconds. Our DDPG agent was trained for approximately

Symbol	Description	Value
l_r	Learning rate	0.001
γ	Reward discount factor	0.95
N_D	Size of the replay buffer	2000
B	Training batch size	32
τ	Soft target update rate	0.001
θ_1	Parameter in Ornstein–Uhlenbeck process	0.15 s^{-1}
σ_1	Parameter in Ornstein–Uhlenbeck process	$0.20 \text{ s}^{-0.5}$

¹. θ_1 and σ_1 were determined according to the suggestion in (Lillicrap et al., 2015).

Table 2: Hyperparameters used in the simulation.

3000 episodes, with each episode containing 1000 time steps.

After training a purely DDPG car-following agent, we use the practical experience replay buffer to continue training the agent. This extra training process lasts approximately 2500 episodes. It is worth mentioning that in the continuing training process, the agent will not update its policy with the experience from interacting with the simulation environment, but only with the practical experience buffer.

5. Evaluation and discussion

We apply the proposed methods and train an autonomous driving agent in the designed driving scenarios. Afterward, methods were evaluated on the other set of scenarios.

5.1. Evaluation with a leader trajectory from real-world driving dataset

After the training process discussed in Section 4.4, we got two types of DRL agents, one is the agent that relies solely on the DRL algorithms and interaction with the simulation environment to update the policy network. Another agent consists of two stages of learning: the first stage is the common DRL training identical to the first type of agent and the second stage is to extract some good driving behaviors of human drivers by learning from the real driving dataset in the experience replay buffer as discussed in Section 3. To evaluate the performance of the trained two-stage DDPG agent follower, we use one leader trajectory from the real driving dataset by Punzo et al. (2005) that was not used in training. This leader trajectory is published from ROS to the leading vehicle in CARLA simulator using the control neural network in Section 4.3. The result is shown in Figure

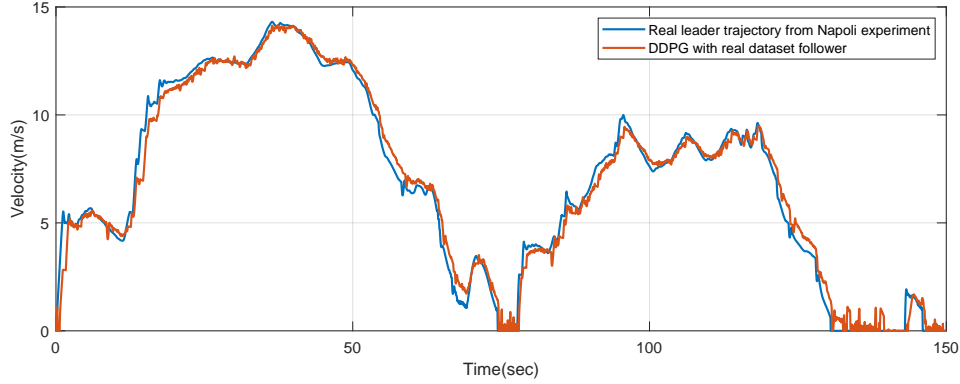
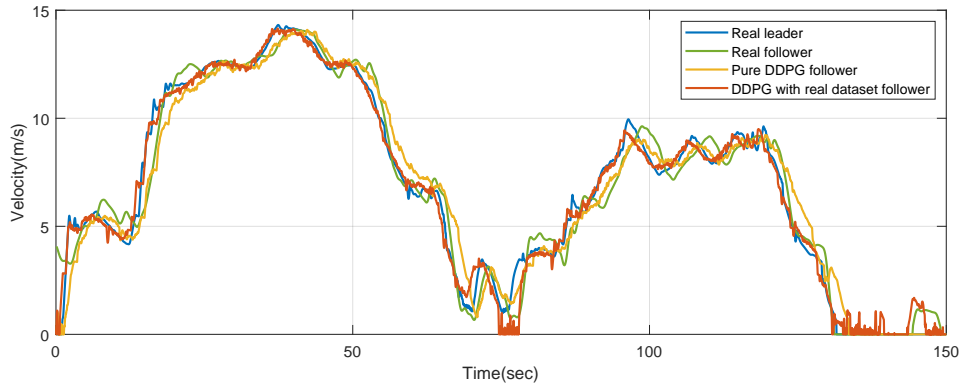


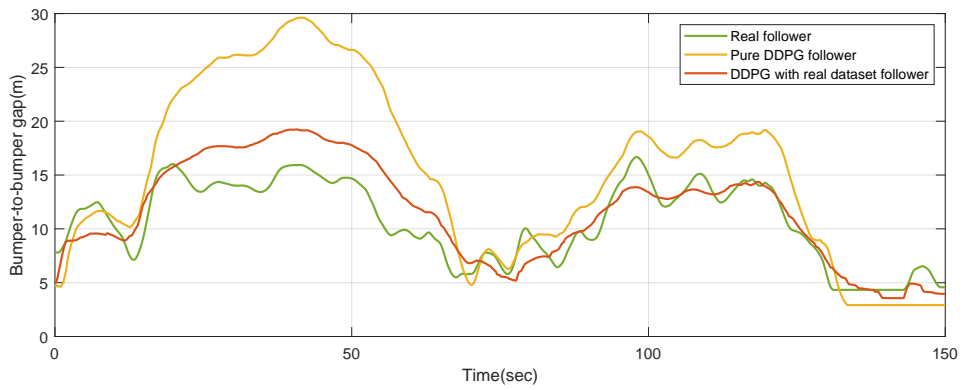
Figure 8: The velocity trajectory of the DDPG follower with human experience from real driving datasets, following a real velocity trajectory from Napoli datasets.

8. We see that the trained two-stage agent can follow the trajectory of the leading vehicle, whether it is in acceleration, deceleration, or standstill phases. Noticing that during the standstill phases such as ($T \in [75s, 80s]$) and ($T \in [130s, 140s]$), when the leader was waiting for the traffic light in the signalized intersection, the DDPG with human experience agent still keeps small velocity to approach the leader with safe distance, and wait for the traffic light turning green. This anticipation driving behavior does not appear in the pure DDPG agent.

To verify that the agent we trained learned human driving behavior from real data, we compare two different DRL agents and the real follower in the real driving dataset. Since in Hart et al. (2021), with the same reward function as in this paper, the DDPG agent already behaves similarly or in some cases better than the IDM model, we will not include IDM in comparison. As illustrated in Figure 9, the velocity trajectory and the bumper-to-bumper distance between each follower and their leader is used. From this figure, we see that the DDPG with human experience follower does extract some human driving behavior from the real data. The pure DDPG agent tends to maintain a large distance from the leader during the high-speed driving phase ($T \in [15s, 65s]$ and $T \in [90s, 125s]$), but in the low-speed or standstill phase ($T \in [130s, 140s]$), it is accustomed to keep a short distance to the leader. However, this is not the driving behavior we want. In the high-speed driving phase, for driving efficiency, we hope that the vehicle maintains an appropriate distance while ensuring safety. The agent trained through the reward function shows a more passive driving style at high speeds and tends to be safe, therefore keeping a larger distance from the leader. However, in the standstill



(a) Speed comparison of different follower



(b) Bumper-to-bumper gap comparison of different follower

Figure 9: The evaluation results by following a real leader trajectory from Napoli datasets for pure DDPG agent and DDPG agent with human experience.

phase, the agent tends to keep a shorter distance from the leader than the usual human driver, which is a potential safety risk for not only the passenger of the ego vehicle but also for the leading vehicle driver.

After learning from the real human driving data, the DDPG agent modified its driving policy and tends to drive much closer to the leader compared with the pure DDPG agent, and during the standstill phase, the two-stage DDPG agent tried to stand farther to the leader.

5.2. Evaluation with self-defined leading vehicle speed profile

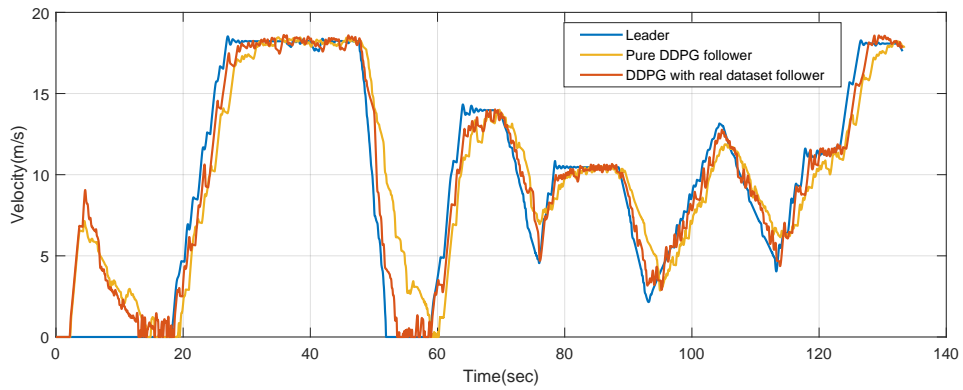
Next, we designed a leading vehicle speed profile that accounts for specific behavior not seen in the Napoli dataset. First, we define a velocity trajectory for the leading vehicle with some safety-critical and common driving behavior. Figure 10 illustrates the comparison of the performance of DDPG agent and DDPG agent with human experience from real-world driving datasets.

The initial gap between followers and leader is 50 meters, and the initial velocity of each follower is 0 m/s. Both followers accelerate from a standstill state as they realize the big distance to the leader. By approaching the leader, both followers reduce their velocity to obtain a safe distance. As the leading vehicle starts to accelerate from $T = 18$ s and reaches the velocity of 18 m/s, both followers follow this change. The pure DDPG agent is clearly much passive, needs more reaction time, and keeps a bigger distance during the constant velocity driving stage. Due to learning from the human driving behavior, the two-stage DDPG follower has a shorter reaction time and keeps much closer to the leader, which improves the driving efficiency.

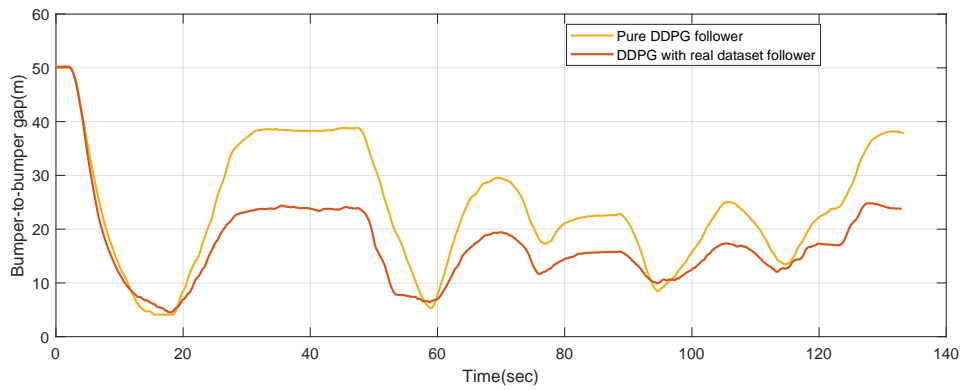
From $T = 48$ s, the leader performs safety-critical braking with the deceleration of -5 m/s^2 until it stops. Our two-stage DDPG follower notices this braking timely and starts to decelerate accordingly and keeps the safe distance all the time. Same as the starting point, the pure DDPG follower can not sense this braking opportunely and leads to a smaller distance to the leader. Afterward, the leader drives with some common accelerate and decelerate scenarios, and the two-stage follower is able to keep an appropriate distance than the pure DDPG follower.

6. Conclusion and outlook

In this study, we proposed a so-called two-stage DDPG method to combine the real-world human driving dataset with DRL method to obtain a car-following agent which has human experience. With this approach, the agent can improve its



(a) Speed comparison of different follower



(b) Bumper-to-bumper gap comparison of different follower

Figure 10: The evaluation results by following an external leader trajectory for pure DDPG agent and DDPG agent with human experience.

driving policy by extracting the good behaviors from real-world human demonstrations, such as anticipation in a signalized intersection. This will help the autonomous agent more adapt to the real-world traffic environment. Moreover, we also proposed a framework that uses ROS and hyper-realistic autonomous driving simulator CARLA together to overcome the communication problem for car-following task. With this framework, the agent is able to obtain all the information from other vehicles, for instance, position, velocity, acceleration, etc. We used a small control network to connect to the policy network from DDPG for generalization. This control network can be retrained repeatedly for different types of vehicles whether in reality or simulation. Therefore, the trained DDPG networks can be reused many times. To the best of our knowledge, this is the first time that the CARLA ROS communication method and the general control network are used for DRL in CARLA.

To evaluate the results, we designed different driving scenarios to test how the two-stage DDPG agent improved its driving ability. All the scenarios showed that the two-stage DDPG agent was superior to the pure DDPG agent in terms of safety and driving efficiency. The proposed framework with CARLA-ROS communication made the car-following task with DRL in CARLA very easy to train and evaluate.

Although our research showed that combining the real-world human demonstrations improved the driving ability of the DDPG agent, there are still some suboptimal issues. One of them is that we calculate the reward for the actions in the real driving dataset based on the expert experience reward function. This cannot fully represent the behavior of the real driver, since this reward function is not the internal reward function when human drives in real-world traffic. A better solution is to use Inverse Reinforcement Learning (IRL) to obtain the internal reward function from the human driver. This will be discussed in the forthcoming paper.

Acknowledgement

This work was funded by ScaDS.AI (Center for Scalable Data Analytics and Artificial Intelligence) Dresden/Leipzig. We thank Vincenzo Punzo for providing the experimental car-following dataset.

References

Akhloufi, M.A., Arola, S., Bonnet, A., 2019. Drones chasing drones: Reinforcement learning and deep search area proposal. *Drones* 3, 58.

- Barocas, S., Hardt, M., Narayanan, A., 2017. Fairness in machine learning. Nips tutorial 1, 2017.
- Bojarski, M., Del Testa, D., Dworakowski, D., Firner, B., Flepp, B., Goyal, P., Jackel, L.D., Monfort, M., Muller, U., Zhang, J., et al., 2016. End to end learning for self-driving cars. arXiv preprint arXiv:1604.07316 .
- Codevilla, F., Müller, M., López, A., Koltun, V., Dosovitskiy, A., 2018. End-to-end driving via conditional imitation learning, in: 2018 IEEE International Conference on Robotics and Automation (ICRA), IEEE. pp. 4693–4700.
- Codevilla, F., Santana, E., López, A.M., Gaidon, A., 2019. Exploring the limitations of behavior cloning for autonomous driving, in: Proceedings of the IEEE/CVF International Conference on Computer Vision, pp. 9329–9338.
- Dosovitskiy, A., Ros, G., Codevilla, F., Lopez, A., Koltun, V., 2017. CARLA: An open urban driving simulator, in: Proceedings of the 1st Annual Conference on Robot Learning, pp. 1–16.
- Dupuis, M., Strobl, M., Grezlikowski, H., 2010. Opendrive 2010 and beyond—status and future of the de facto standard for the description of road networks, in: Proc. of the Driving Simulation Conference Europe, pp. 231–242.
- Dworak, D., Ciepiela, F., Derbisz, J., Izzat, I., Komorkiewicz, M., Wójcik, M., 2019. Performance of lidar object detection deep learning architectures based on artificially generated point cloud data from carla simulator, in: 2019 24th International Conference on Methods and Models in Automation and Robotics (MMAR), IEEE. pp. 600–605.
- Gazis, D.C., Herman, R., Rothery, R.W., 1961. Nonlinear follow-the-leader models of traffic flow. Operations research 9, 545–567.
- Gómez-Huélamo, C., Del Egado, J., Bergasa, L.M., Barea, R., López-Guillén, E., Arango, F., Araluce, J., López, J., 2020. Train here, drive there: Simulating real-world use cases with fully-autonomous driving architecture in carla simulator, in: Workshop of Physical Agents, Springer. pp. 44–59.
- Gu, S., Holly, E., Lillicrap, T., Levine, S., 2017. Deep reinforcement learning for robotic manipulation with asynchronous off-policy updates, in: 2017 IEEE international conference on robotics and automation (ICRA), IEEE. pp. 3389–3396.

- de Haan, P., Jayaraman, D., Levine, S., 2019. Causal confusion in imitation learning. *Advances in Neural Information Processing Systems* 32, 11698–11709.
- Hanin, B., Rolnick, D., 2018. How to start training: The effect of initialization and architecture. *arXiv preprint arXiv:1803.01719* .
- Hart, F., Okhrin, O., Treiber, M., 2021. Formulation and validation of a car-following model based on deep reinforcement learning. *arXiv preprint arXiv:2109.14268* .
- He, Y., Zhao, N., Yin, H., 2017. Integrated networking, caching, and computing for connected vehicles: A deep reinforcement learning approach. *IEEE Transactions on Vehicular Technology* 67, 44–55.
- Hellmund, A.M., Wirges, S., Taş, Ö.Ş., Bandera, C., Salscheider, N.O., 2016. Robot operating system: A modular software framework for automated driving, in: *2016 IEEE 19th International Conference on Intelligent Transportation Systems (ITSC)*, IEEE. pp. 1564–1570.
- Huang, Z., Wu, J., Lv, C., 2021. Efficient deep reinforcement learning with imitative expert priors for autonomous driving. *arXiv preprint arXiv:2103.10690* .
- Isele, D., Rahimi, R., Cosgun, A., Subramanian, K., Fujimura, K., 2018. Navigating occluded intersections with autonomous vehicles using deep reinforcement learning, in: *2018 IEEE International Conference on Robotics and Automation (ICRA)*, IEEE. pp. 2034–2039.
- Kalman, R.E., 1960. A new approach to linear filtering and prediction problems .
- Kikuchi, S., Chakroborty, P., 1992. Car-following model based on fuzzy inference system. *Transportation Research Record* , 82–82.
- Kim, D., 1999. Normalization methods for input and output vectors in backpropagation neural networks. *International journal of computer mathematics* 71, 161–171.
- Lillicrap, T.P., Hunt, J.J., Pritzel, A., Heess, N., Erez, T., Tassa, Y., Silver, D., Wierstra, D., 2015. Continuous control with deep reinforcement learning. *arXiv preprint arXiv:1509.02971* .

- Lin, L.J., 1992. Self-improving reactive agents based on reinforcement learning, planning and teaching. *Machine learning* 8, 293–321.
- Liu, H., Huang, Z., Lv, C., 2021. Improved deep reinforcement learning with expert demonstrations for urban autonomous driving. *arXiv preprint arXiv:2102.09243* .
- Mnih, V., Kavukcuoglu, K., Silver, D., Graves, A., Antonoglou, I., Wierstra, D., Riedmiller, M., 2013. Playing atari with deep reinforcement learning. *arXiv preprint arXiv:1312.5602* .
- Mnih, V., Kavukcuoglu, K., Silver, D., Rusu, A.A., Veness, J., Bellemare, M.G., Graves, A., Riedmiller, M., Fidjeland, A.K., Ostrovski, G., et al., 2015. Human-level control through deep reinforcement learning. *nature* 518, 529–533.
- Ngai, D.C.K., Yung, N.H.C., 2011. A multiple-goal reinforcement learning method for complex vehicle overtaking maneuvers. *IEEE Transactions on Intelligent Transportation Systems* 12, 509–522.
- Niranjan, D., VinayKarthik, B., et al., 2021. Deep learning based object detection model for autonomous driving research using carla simulator, in: *2021 2nd International Conference on Smart Electronics and Communication (ICOSEC)*, IEEE. pp. 1251–1258.
- Nosrati, M.S., Abolfathi, E.A., Elmahgiubi, M., Yadmellat, P., Luo, J., Zhang, Y., Yao, H., Zhang, H., Jamil, A., 2018. Towards practical hierarchical reinforcement learning for multi-lane autonomous driving .
- Punzo, V., Formisano, D.J., Torrieri, V., 2005. Nonstationary kalman filter for estimation of accurate and consistent car-following data. *Transportation research record* 1934, 2–12.
- Quigley, M., Conley, K., Gerkey, B., Faust, J., Foote, T., Leibs, J., Wheeler, R., Ng, A.Y., et al., 2009. Ros: an open-source robot operating system, in: *ICRA workshop on open source software*, Kobe, Japan. p. 5.
- Ravi Kiran, B., Roldao, L., Irastorza, B., Verastegui, R., Suss, S., Yogamani, S., Talpaert, V., Lepoutre, A., Trehard, G., 2018. Real-time dynamic object detection for autonomous driving using prior 3d-maps, in: *Proceedings of the European Conference on Computer Vision (ECCV) Workshops*, pp. 0–0.

- Sallab, A.E., Abdou, M., Perot, E., Yogamani, S., 2016. End-to-end deep reinforcement learning for lane keeping assist. arXiv preprint arXiv:1612.04340 .
- Silver, D., Huang, A., Maddison, C.J., Guez, A., Sifre, L., Van Den Driessche, G., Schrittwieser, J., Antonoglou, I., Panneershelvam, V., Lanctot, M., et al., 2016. Mastering the game of go with deep neural networks and tree search. *nature* 529, 484–489.
- Silver, D., Hubert, T., Schrittwieser, J., Antonoglou, I., Lai, M., Guez, A., Lanctot, M., Sifre, L., Kumaran, D., Graepel, T., et al., 2017. Mastering chess and shogi by self-play with a general reinforcement learning algorithm. arXiv preprint arXiv:1712.01815 .
- Thrun, S., Montemerlo, M., Dahlkamp, H., Stavens, D., Aron, A., Diebel, J., Fong, P., Gale, J., Halpenny, M., Hoffmann, G., et al., 2006. Stanley: The robot that won the darpa grand challenge. *Journal of field Robotics* 23, 661–692.
- Tran, L.A., Le, M.H., 2019. Robust u-net-based road lane markings detection for autonomous driving, in: 2019 International Conference on System Science and Engineering (ICSSE), IEEE. pp. 62–66.
- Treiber, M., Hennecke, A., Helbing, D., 2000. Congested traffic states in empirical observations and microscopic simulations. *Physical review E* 62, 1805.
- Treiber, M., Kesting, A., 2017. The intelligent driver model with stochasticity—new insights into traffic flow oscillations. *Transportation research procedia* 23, 174–187.
- Uhlenbeck, G.E., Ornstein, L.S., 1930. On the theory of the brownian motion. *Physical review* 36, 823.
- Vecerik, M., Hester, T., Scholz, J., Wang, F., Pietquin, O., Piot, B., Heess, N., Rothörl, T., Lampe, T., Riedmiller, M., 2017. Leveraging demonstrations for deep reinforcement learning on robotics problems with sparse rewards. arXiv preprint arXiv:1707.08817 .
- Wang, P., Chan, C.Y., de La Fortelle, A., 2018. A reinforcement learning based approach for automated lane change maneuvers, in: 2018 IEEE Intelligent Vehicles Symposium (IV), IEEE. pp. 1379–1384.
- Wiedemann, R., 1974. Simulation des strassenverkehrsflusses. .